Hindawi Publishing Corporation
Mathematical Problems in Engineering
Volume 2015, Article ID 457303, 14 pages
http://dx.doi.org/10.1155/2015/457303

Research Article

A New Method to Optimize Semiactive Hybrid Energy Storage System for Hybrid Electrical Vehicle by Using PE Function

Cong Zhang,[1] Haitao Min,[1] Yuanbin Yu,[1] Qingnian Wang,[1] and Huanli Sun[2]

[1]*State Key Laboratory of Automotive Simulation and Control, Jilin University, Changchun 130022, China*
[2]*FAW R&D Center, Changchun 130022, China*

Correspondence should be addressed to Yuanbin Yu; yyb@jlu.edu.cn

Received 9 June 2015; Revised 29 August 2015; Accepted 2 September 2015

Academic Editor: Weiguo Xia

Although both battery and super-capacitor are important power sources for hybrid electric vehicles, there is no accurate configuration theory to match the above two kinds of power sources which have significantly different characteristics on energy and power storage for the goal of making good use of their individual features without size wasting. In this paper, a new performance is presented that is used for analysis and optimal design method of battery and super-capacitor for hybrid energy storage system of a parallel hybrid electrical vehicle. In order to achieve optimal design with less consumption, the power-energy function is applied to establish direct mathematical relationship between demand power and the performance. During matching process, firstly, three typical operating conditions are chosen as the basis of design; secondly, the energy and power capacity evaluation methods for the parameters of battery and super-capacitor in hybrid energy storage system are proposed; thirdly, the mass, volume, and cost of the system are optimized simultaneously by using power-energy function. As a result, there are significant advantages on mass, volume, and cost for the hybrid energy storage system with the matching method. Simulation results fit well with the results of analysis, which confirms that the optimized design can meet the demand of hybrid electric vehicle well.

1. Introduction

The energy storage system (ESS) is taken as the auxiliary power source to alleviate load shifting and improve fuel economy and emission on hybrid electric vehicles (HEVs) [1–3]. Li-ion battery is widely used in these applications owing to its high energy density, proven safety, and competitive cost [4, 5]. Super-capacitor (SC) with long lifecycle and high energy efficiency is evaluated in automotive industry and academia for hybrid energy storage system (HESS) [6], in cooperation with battery and DC/DC converter [7–9]. According to above literatures, the first potential benefit of HESS is represented by the power loss reduction in the energy storage. In fact, the energy efficiency of SC is higher than that of battery, especially at significant currents. Moreover, SC allows regeneration even when the vehicle is working in critical ambient conditions (i.e., at low temperatures) [10–12], in which the battery cannot operate in regenerative mode [13]. The key issue with HESS optimization is how to effectively protect the battery by using SC in order to improve system efficiency and prolong service life of battery [14]. Three main factors should be considered: the HESS topology, battery and SC size, and control strategy (CS) [15].

Regarding the HESS topology, there are three major types: passive, semiactive, and fully active. The passive HESS is the simplest topology because the battery and SC package are connected in parallel and coupled directly to the DC bus [11, 16]. In this topology, the SC works as a low-pass filter for battery. Although no additional electronic components are needed, the filtering effect inherently depends on the resistance of the battery/SC as well as the capacity because of the difference of voltage characteristics between battery and SC. Nevertheless, from the costs and the actual effects, passive HESS is rarely used in practical engineering. On the contrary, because the fully active HESS employs two DC/DC converters and additional control circuit, this topology demands compromise in terms of cost, mass, volume, efficiency, and simplicity [15, 17]. At the same time, the losses in DC/DC should not be ignored [18]. Based on the results of studies [19, 20], the semiactive HESS is favored to be the most popular

topology, which only employs one DC/DC converter. It is a good tradeoff between performances, cost, and complexity. In additional, most control strategies can be implemented in this topology. Taking into account the need to charge/discharge frequently and the losses in DC/DC, the topology similar to the one used in [21] with a smaller DC/DC in comparison with the conventional HESS, is regarded as a case study in this paper. The SC provides energies directly to the motor, and battery with DC/DC will participate into work according to the state of SC when necessary.

For optimal energy management, a variety of online CSs for HESS have been empirically designed and discussed in recent literatures, such as the "all or nothing" [1], rule-based [19], filtration based [20], model predictive [22], fuzzy logic CSs [18, 23], efficient CS [24], and minimizing total fuel consumption [25]. Furthermore, under certain driving cycle and configurations, the offline CSs such as dynamic programming (DP) and Pontryagin's minimum principle algorithms could find the global optimization solution. Santucci et al. [21] propose a DP algorithm including a simplified battery aging model. Vinot et al. [26] use Pontryagin's minimum principle to reduce the RMS of the battery current.

Besides the control strategy, the configuration is another key factor contributing to the performance of HESS. Schupbach et al. [16] use P/E ratio as central indices throughout the design, which should be adjusted to match the ratio of the maximum power to the maximum energy of HESS. However, because of the complexity of the active control system and the different features between the batteries and the SC, the P/E ratio does not accurately describe the power and energy capability of the active-combination energy storage system (ACES) or the fluctuating power demand from the HEV with some arguments [27]. Considering the interaction between the CS and configuration, Miller et al. [20] present a codesign philosophy to get the optimal solution; cost and size ratios are selected as two factors to determine the HESS with maximum energy storage capacity. A set of optimal size ratio under various fixed costs is thus searched, and the cost and size ratio with the largest value of energy is globally searched to be the optimal solution of system design; the philosophy is also used by Hung and Wu [27]. Song et al. [28] utilize the dynamic programming (DP) approach to deal with the integrated optimization problem for deriving the best configuration and energy split strategies of a HESS for an electric city bus. It is shown that the life cycle cost of the HESS initially decreases rapidly with the addition of SC, though the rate of this reduction decreases as the amount of SC increases. Hung and Wu [27] develop a simple but innovative integrated optimization approach (IOA) for deriving the best solutions of component sizing and CSs of a HESS. The simulation results show that 6% of the total energy can be saved in the IOA case compared with the original system in two driving cycles: ECE and UDDS, and two vehicle weights, respectively.

By using DP, the optimal HESS solution in terms of a specific vehicle and driving cycle can be found, which has been proven crucial for saving energy, reducing cost, reaching high overall efficiency, and reducing the peak and root mean square (RMS) values of the battery current to extend its life span [1, 29]. However, this optimization problem is computationally expensive because a lot of possibilities exist when all the factors are alterable. Therefore their use in practical applications is challenging [30]. As a result, only one factor (e.g., the HESS topology or CS) is considered in most published literature [31], and only a few focus on two or more different factors simultaneously [28].

To present a widely applicable and mathematical method to analyze the design process, the PE function and PE density matrix which is extracted from the working data of HESS used in an HEV are proposed in [32]. The minimum matched ACES under optimal power split strategy which can meet the requirements is founded. In the meantime, the efficiency of the system can also be estimated. In the meantime, considering energy loss as the evaluation indices, it comes to the conclusion that the energy loss increases firstly then declines with the increasing trend of SC capacity. However, it only discusses the capacity relation between battery and SC qualitatively, which is not sufficient enough to guide the engineering practice quantitatively.

Overall, considering the existing research either time-consuming and cycle dependent or only suboptimized, there is no efficient and practical applicable method in multiobjective optimization when factors are alterable. This paper considers the factors such as charge/discharge capacity, size, life cycle, and DC/DC efficiency which could optimize the parameter configuration effectively.

The objectives of this paper are the following:

(i) to extract the power and energy demands of ESS for a case study parallel HEV along conditions which are not cycle dependent;

(ii) to propose appropriate indices (i.e., energy capacity for charging/discharging) as calculation basis of performance parameters;

(iii) to present a novel and practical method in multiobjective optimization (i.e., mass, volume, and cost of HESS) by using PE function. Further optimization can be done combined with the research results of [21, 32];

(iv) to verify the accuracy of analysis through simulation.

This paper is based on several functional requirements of HESS for HEV. The charge/discharge capacity of HESS which is needed to meet has been proposed through modeling and simulation. According to the characteristic of vehicle operating, the power and energy density of battery and SC are recalculated based on the charge/discharge capacity requirements. Multiobjective optimization of HESS is proposed including mass, volume, and cost.

2. Power Demand of HESS in HEV

In this paper the HEV is a parallel power system, and the configuration is shown in Figure 1. The HESS comprises SC package, battery package, DC/DC converter, engine, ISG motor, electronic controlling clutch, main drive motor (M), and transmission unit. Accessories such as air conditioning and vacuum booster systems are electrically driven. The battery and SC package are combined in parallel through the

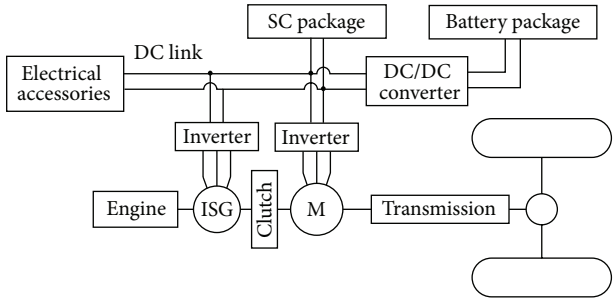

Figure 1: Configuration diagram of the HEV power system.

Table 1: HEV parameters.

Parameter	Value
Total mass	18000 kg
Frontal area	7.3
Wind resistance coefficient	0.78
Rolling resistance coefficient	0.01
Engine	110 kw
ISG motor	20 kw
Main drive motor	100 kw

DC/DC converter to supply power to the main drive motor to support the regular operations of the system. The HESS is required to have the ability to drive the vehicle, supply enough power, and restore the regenerative braking energy efficiently. The parameters of the HEVs are listed in Table 1.

For the high voltage DC bus of the ESS, the design range of operating voltage is 250–400 V. In the case that the available energy of both the batteries and the SC is 50%, the demanded power under the following three conditions should be satisfied by the ESS [18–20].

(i) Power up in EV mode is the first condition. In the start phase, the power supplied by single motor is used to start the entire HEV without engine working. When operating in city, public buses have to stop and start repeatedly. Public HEV bus could cancel idle mode by shutting the engine off automatically when the vehicle halts. However, accessories such as the vacuum booster and air conditioner still depend on the ESS to supply the energy. Therefore, the ESS is required to maintain the functionality of those accessories during the short period like idle and then still have the ability to power up the HEV using electricity only. The sample used in this study should have the ability to power up in EV mode after halting for 3 minutes and then speeds up to 20 km/h. The demanded power for the ESS during this process is shown in Figure 2.

(ii) For acceleration, HEV requires the motor to provide high auxiliary power during acceleration, meaning that the ESS must have a certain level of discharging ability. The sample vehicle in this study is required to accelerate from 0 to 50 km/h within 20 seconds. The demanded power for the ESS during this process is shown in Figure 3.

(iii) During regenerative braking, the main drive motor should supply the force for braking, which converts the vehicle's kinetic energy to electrical energy that would be stored in the ESS. The ESS is required to have a certain level of charging ability. The sample used in this study must be able to fulfill a regenerative brake while traveling speed is reduced from 50 km/h to standstill. The demanded power for the ESS during this process is shown in Figure 4.

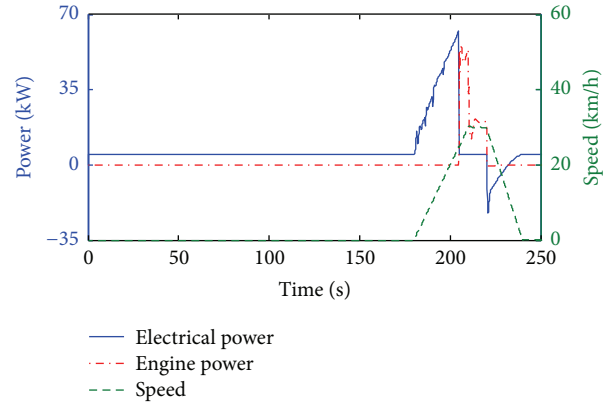

Figure 2: Demanded power for the power system of the HEV in EV mode.

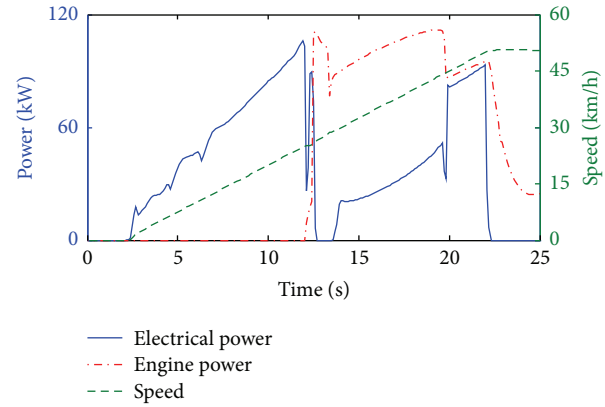

Figure 3: Demanded power for the power system of the HEV during acceleration.

3. Evaluation Method for the ESS Performance of the HEV

The performance requirements for the ESS are reflected in two aspects: (i) power capacity; (ii) energy capacity during charging and discharging. The application environment of the HEVs' ESS is discussed and a method is proposed to calculate the ability of the batteries and SCs on the two performance requirements in this section. The parameters for the Li-ion battery and the SC are listed in Table 2 [12, 32].

HEVs have higher demanded power but lower energy demand for the ESS. Li-ion battery has high energy density but low power density. Therefore, the energy of the Li-ion battery used in HEVs is usually more than required [33–36]. In order to achieve good performance characteristics over lifespan, the state of charge (SOC) of the battery should be

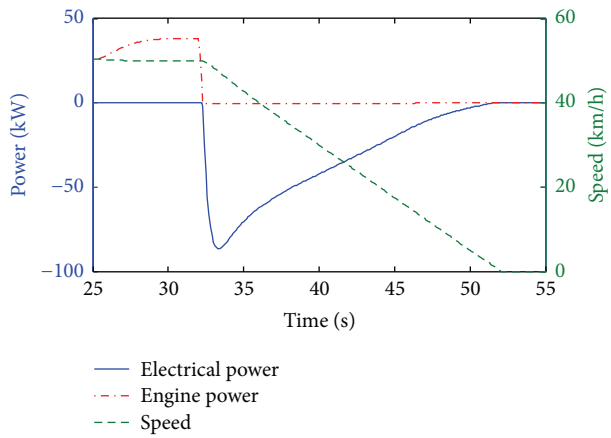

Figure 4: Demanded power for the power system of the HEVs during braking.

Table 2: Single parameters for the Li-ion battery and SC.

Parameter	Li-ion battery	SC
Cell capacity	8 Ah	1500 F
Internal resistance/mΩ	7	0.47
Voltage range/V	2.5–3.65	0–2.7
Weight/g	260	320
Volume/L	0.18	0.33
Cost/$	10	14

controlled in the range of 0.4–0.6. So it is generally controlled within that range to prolong the battery life [37].

Based on previous studies [38], there is only mild variation during charging/discharging when the SOC is 0.4–0.6; therefore, it can be treated as a constant. When the SOC is 0.4, the maximum continuous discharging power of the battery is the minimum value. That value is denoted as $P_{\text{BATlimit}D}$, which is the limit of the battery's discharging power during operating. When the SOC is 0.6, the maximum continuous charging power of the battery is the smallest value. That value is denoted as $P_{\text{BATlimit}C}$, which is the limit of the battery's charging power. Based on the charging and discharging performance requirement for ESS, 50% of the battery energy could be set as the balance point for charging and discharging [31]. And the battery SOC is chosen as 0.4–0.6 in

$$E_{\text{BAT}} = C_{\text{BAT}}\text{OCV}_{\text{BAT}}\,(0.6 - 0.4) \times 50\%, \tag{1}$$

where E_{BAT} is the energy capacity for charging and discharging (Wh); OCV_{BAT} is the open-circuit voltage (V); and C_{BAT} is the battery capacity (Ah). Based on the principle above, the power and energy performance parameters of the battery in HEV (with the cell parameters in Table 2) can be ensured in Table 3.

SCs are used in HEV because of their high power density, efficiency, low internal resistance, and long operational lifespan [39]. The efficiency of SC during charging and discharging is reduced with charging/discharging power increasing. For HEVs, when calculating the power limits

Table 3: Performance parameters of the lithium battery cell.

Parameter	Value
OCV/V	3.2
Charging power limit/W	64
Discharging power limit/W	128
Energy capacity/Wh	2.6

during charging/discharging, certain efficiency of the SC should be guaranteed [40, 41]. The efficiency can be calculated using the internal resistance model as shown in

$$\begin{aligned}\text{Discharging: } \eta_{\text{UC}} &= \frac{\text{OCV}_{\text{UC}} - IR_{\text{UC}}}{\text{OCV}_{\text{UC}}},\\ \text{Charging: } \eta_{\text{UC}} &= \frac{\text{OCV}_{\text{UC}}}{\text{OCV}_{\text{UC}} + IR_{\text{UC}}},\end{aligned} \tag{2}$$

where η_{UC} represents efficiency; OCV_{UC} is the open-circuit voltage; I is the current; and R_{UC} is the internal resistance. In this study, the lowest limit for efficiency is set as 0.9 to calculate the current limit of the SC during charging/discharging. This is shown in

$$\begin{aligned}\text{Discharging: } I_{\text{limit}D} &= \frac{\text{OCV}_{\text{UC}}}{10R_{\text{UC}}},\\ \text{Charging: } I_{\text{limit}C} &= \frac{\text{OCV}_{\text{UC}}}{9R_{\text{UC}}},\end{aligned} \tag{3}$$

where $I_{\text{limit}D}$ and $I_{\text{limit}C}$ refer to the current limits of the SC during discharging/charging, respectively. Using the terminal voltage and current limits for charging/discharging, the power limit of the SC during charging/discharging can be calculated on the basis of the efficiency considerations for the HEV. This is shown in

$$\begin{aligned}\text{Discharging: } P_{\text{UClimit}D} &= \frac{9}{100}\frac{\text{OCV}_{\text{UC}}^2}{R_{\text{UC}}},\\ \text{Charging: } P_{\text{UClimit}C} &= \frac{10}{81}\frac{\text{OCV}_{\text{UC}}^2}{R_{\text{UC}}},\end{aligned} \tag{4}$$

where $P_{\text{UClimit}D}$ and $P_{\text{UClimit}C}$ refer to the power limit of the SC during discharging/charging, respectively.

As shown in the equations above, the power limit of the SC in HEVs based on the efficiency consideration is determined by the internal resistance and open-circuit voltage [42]. The former is an intrinsic property, whereas the latter has a linear relationship with electricity. SCs are placed at both ends of the motor in parallel. Their operating range is 250–400 V, with a corresponding range of a single working voltage at 1.67–2.67 V. The open-circuit voltage of the SC can also be approximated at 1.67–2.67 V. In this study, OCV_{UC} is set at 1.67 V and fed into (4). Then the power limit of the SC under worst operating condition during charging/discharging is obtained. This value is then used as the power limit of the SC in HEV during charging/discharging [6].

Table 4: Performance parameters of the SC.

Parameter	Value
OCV/V	1.67–2.67
Charging power limit/W	732
Discharging power limit/W	564
Energy capacity/Wh	0.45

Table 5: Energy densities of the batteries and SCs.

Parameter	Battery	SC
Power mass ratio when charging/discharging/W/kg	246/492	2287/1762
Power volume ratio when charging/discharging/W/L	355/710	2218/1709
Power cost ratio when charging/discharging/W/$	6.4/12.8	52.3/40.3
Energy mass ratio/Wh/kg	10	1.4
Energy volume ratio/Wh/L	14.6	1.36
Energy cost ratio/Wh/$	0.26	0.032

Equation (5) is the energy calculation for SC. So the energy capacity of the SC can be calculated using voltage range, as shown in

$$E = \frac{1}{2}\mathrm{CU}^2 \tag{5}$$

$$E_{\mathrm{UC}} = \frac{1}{2}C_{\mathrm{UC}}\left(2.67^2 - 1.67^2\right) \times 50\%, \tag{6}$$

where E_{UC} represents the energy capacity for charging/discharging (Wh). Based on the principle above, the calculated performance of the SC is summarized in Table 4.

The volume, mass, and cost of per unit can be calculated by combining the data from Tables 2–4. The performance of the battery and SC in terms of power and energy is summarized in Table 5.

4. Demanded Power Based Optimal Design for the Performance of HESS

4.1. HESS Configuration. The HESS is the combination of Li-ion battery and SC. The overall performance is determined by the performance of the individual units, as well as the total number used in series [43]. Optimization of the HESS is to decide the cell quantity used in series which can achieve optimal cost, mass, and volume, while ensuring that the performance of the HESS can meet the demand.

As is shown in Figure 5, the SC package is constituted by SC branches which are arranged in parallel at both ends of the motor, with an operating voltage range of 250–400 V. There are two characteristics for the SC package: (i) the wider the range of the operating voltage is, the greater the energy will be; (ii) for the same quantity units, the larger number of units that are arranged in series, the smaller combined capacity of the SC package. Owing to these two characteristics, 150 single SC units are arranged in series to constitute a SC branch. SC

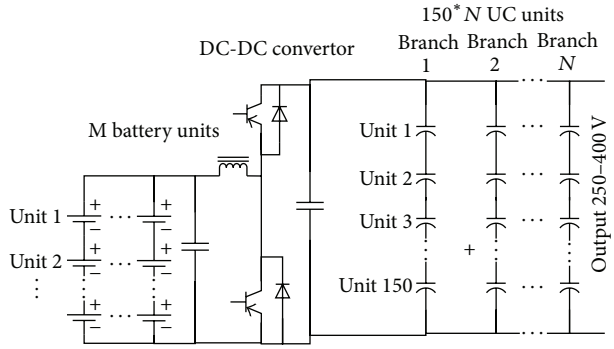

Figure 5: Configuration of the HESS.

branch is treated as a special indivisible unit. N SC branches are grouped in parallel to form the SC package of $150^* N$ units. With a DC/DC converter, the range of operating voltage for a battery unit is 160–260 V. The configuration of M (number of battery units) is flexible and can be arranged in either series or parallel according to the actual requirement.

4.2. Performance Analysis of the HESS. The performance of the HESS refers to its ability to satisfy the demanded power [44]. The performance is determined by the individual performance parameters, including energy capacity and charging/discharging power limits of the battery and SC package. The following three conditions are used to determine whether the HEES can satisfy the demanded power shown below.

(i) P_{required} (demanded power) must be less than the sum of the limits of P_{BATlimit} (battery power) and P_{UClimit} (capacitor power), which is

$$P_{\mathrm{required}} \le \left(P_{\mathrm{UClimit}} + P_{\mathrm{BATlimit}}\right). \tag{7}$$

(ii) SCs must satisfy any demanded power that exceeds the power limits of batteries. However, the integral of P_{UC} (demanded power from SCs) cannot exceed E_{UC} (energy capacity of SCs), which is

$$\int_0^T P_{\mathrm{UC}}dt \le E_{\mathrm{UC}},$$

$$P_{\mathrm{UC}} = \begin{cases} P_{\mathrm{required}} - P_{\mathrm{BATlimit}}, & P_{\mathrm{required}} > P_{\mathrm{BATlimit}}, \\ 0, & P_{\mathrm{required}} \le P_{\mathrm{BATlimit}}. \end{cases} \tag{8}$$

(iii) The energy required for the entire charging/discharging process should be less than the sum of the energy capacity of E_{BAT} (batteries) and E_{UC} (SCs), which is

$$\int_0^T P_{\mathrm{required}}dt \le E_{\mathrm{UC}} + E_{\mathrm{bat}}. \tag{9}$$

To analyze the effect of parameters for the SC and battery package on the performance of the HESS more intuitively, the concept of PE function is introduced. The function is defined as

$$E = F(P), \tag{10}$$

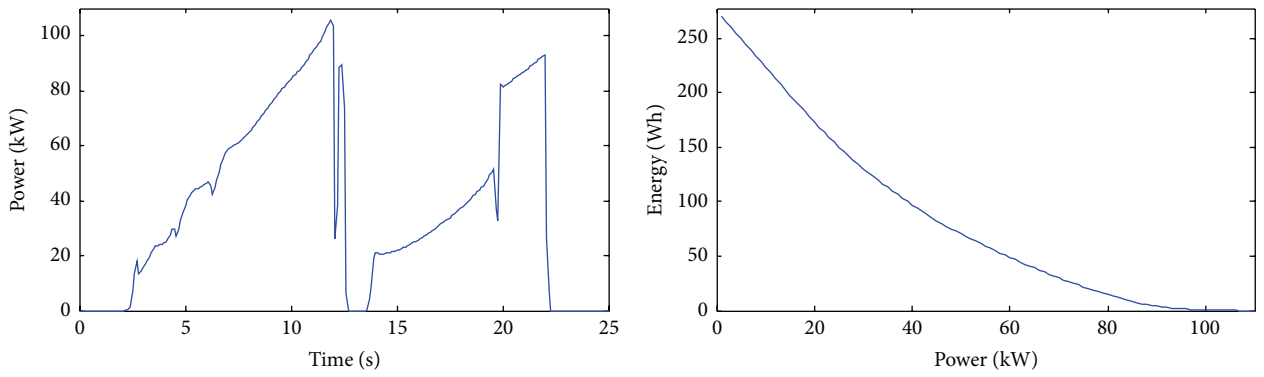

(a) (b)

Figure 6: Demanded power under acceleration and corresponding PE function.

where E represents the energy (Wh) and P represents the power (kW). E in the function represents the integral value of the power versus time whose demand is greater than P. This is the energy value of this power P, as shown in

$$E = \int_0^T f(t)\,dt,$$
$$f(t) = \begin{cases} 0, & P(t) < P, \\ P(t) - P, & P(t) \geq P, \end{cases} \tag{11}$$

where $P(t)$ is the power-demand function in terms of time (kW). This function is known as the PE function. Equations (7)–(9) can be rewritten using this function as follows:

$$F(P_{\text{UClimit}} + P_{\text{BATlimit}}) = 0,$$
$$F(P_{\text{BATlimit}}) \leq E_{\text{UC}}, \tag{12}$$
$$F(0) \leq E_{\text{UC}} + E_{\text{BAT}}.$$

With regard to a particular HESS, it can be observed that the PE function can be used to accurately determine whether the demanded power for charging or discharging process can be met. The demanded power for the HESS under the condition of acceleration is used as an example and shown in Figure 6(a). The corresponding PE function is shown in Figure 6(b).

Based on (12), when the points $(0, E_{\text{BAT}}+E_{\text{UC}})$, $(P_{\text{BATlimit}D}, E_{\text{UC}})$, and $(P_{\text{BATlimit}D} + P_{\text{UClimit}D}, 0)$ shown in Figure 6(b) are not below the PE function curve, the HESS would be able to meet the demanded power. In the PE function figure, the straight line function passing through points $(0, E_{\text{BAT}} + E_{\text{UC}})$ and $(P_{\text{BATlimit}D}, E_{\text{UC}})$ is shown below:

$$y = E_{\text{BAT}} + E_{\text{UC}} - \frac{E_{\text{BAT}}}{P_{\text{BATlimit}D}} x. \tag{13}$$

It is obvious that the gradient of the line is determined by the energy capacity and discharge limit of the battery. Therefore, this is known as the discharge performance line of the batteries. The ratio between the discharge limit and the energy capacity is $R_{\text{BAT\_}D}$ (discharge rate of the batteries). This is shown in

$$R_{\text{BAT\_}D} = \frac{P_{\text{BATlimit}D}}{E_{\text{BAT}}}. \tag{14}$$

Hence, the function of the discharge performance line of the battery can be shown as follows:

$$y = E_{\text{BAT}} + E_{\text{UC}} - \frac{1}{R_{\text{BAT\_}D}} x. \tag{15}$$

Similarly, the straight line through points $(P_{\text{BATlimit}D}, E_{\text{UC}})$ and $(P_{\text{BATlimit}D} + P_{\text{UClimit}D}, 0)$ is known as the discharge performance line of the SC. The ratio between the discharge limit and the energy capacity is $R_{\text{UC\_}D}$ (discharge rate of the SCs). This is shown in

$$R_{\text{UC\_}D} = \frac{P_{\text{UClimit}D}}{E_{\text{UC}}}. \tag{16}$$

Therefore, the function of the discharge performance line of the SC can be shown as follows:

$$y = -\frac{1}{R_{\text{UC\_}D}} x + E_{\text{UC}} + \frac{E_{\text{UC}} P_{\text{BATlimit}D}}{P_{\text{UClimit}D}}. \tag{17}$$

Point $(0, E_{\text{BAT}} + E_{\text{UC}})$ is the intersection of the performance line of the battery with the Y-axis, and with the X-axis it is $(P_{\text{BATlimit}D} + P_{\text{UClimit}D}, 0)$, respectively. Point $(P_{\text{BATlimit}D}, E_{\text{UC}})$ is the intersection between the performance lines of the batteries and SCs, which is also known as the parameter point for the performance of the HESS.

From the performance lines of the batteries and SCs, it can be concluded that the HESS has to satisfy three determining conditions to meet the arbitrary demanded power:

(i) The intersection between the performance line of the battery and Y-axis must be above the intersection between the PE function of demanded power and the Y-axis, as shown in Figure 7(a).

(ii) The intersection between the performance line of the SC and X-axis should be at the right side of the intersection between the PE function of demanded power and X-axis, as shown in Figure 7(b).

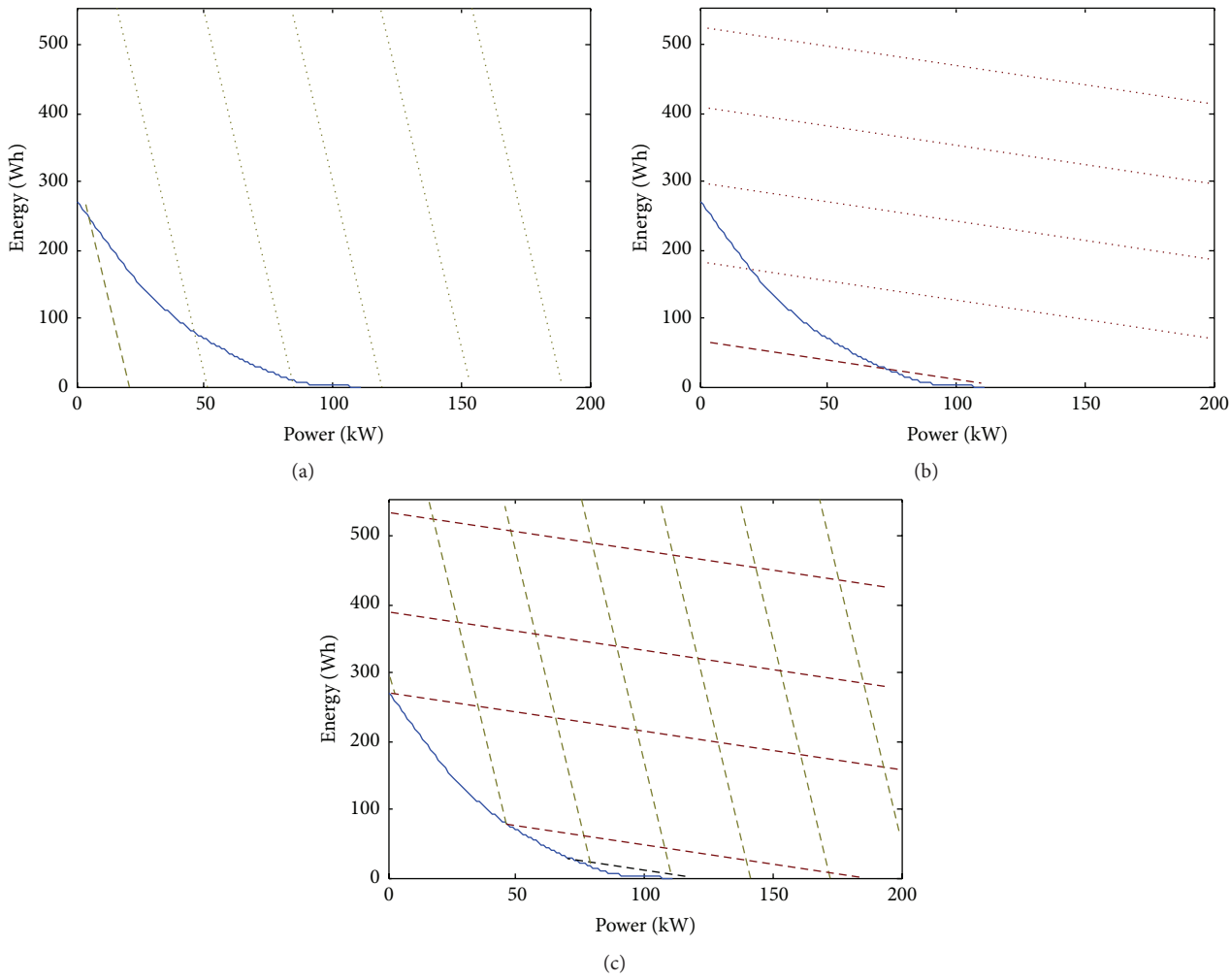

Figure 7: Three determining conditions.

(iii) The intersection between the performance lines of the batteries and SCs should be above the PE function of the demanded power, as shown in Figure 7(c).

As shown in Figure 7(c), each intersection between the performance lines of the batteries and SCs (i.e., each parameter point for the performance of the HESS) corresponds to a possible design proposal in which the HESS is able to meet the demanded power when discharging. Theoretically, Figure 7(c) can be used to obtain all possible methods of setting up the HESS.

Applying the same method, the demanded power and PE function required in EV mode (Figure 8) can be used to determine the range of parameter points for the performance of the HESS when discharging.

The range of parameter points for the performance of HESS when discharging under the EV mode and acceleration mode can be determined by combining the calculation results from acceleration and EV mode. In Figure 9, the region of the right side of the thick black dotted line represents the range of the parameter point $(P_{\text{BATlimit}D}, E_{\text{UC}})$ for the performances of the HESS that meet the demanded power when discharging.

With the same method, the range of parameter points $(P_{\text{BATlimitC}}, E_{\text{UC}})$ for the performance of the HESS that meet the demanded power during charging can be calculated using Figure 10, which shows the demanded power during charging and the corresponding PE function for the regenerative braking process.

The above method is similarly used to, respectively, derive the range of parameter points $(P_{\text{BATlimitC}}, E_{\text{UC}})$ and $(P_{\text{BATlimit}D}, E_{\text{UC}})$ for the performance of the HESS during discharging/charging. Furthermore, (18) are used to indicate the relationship between (i) the power limits of the batteries during charging/discharging and (ii) their energy capacities. This information is then used to derive the range of energy capacities E_{BAT} and E_{UC} (for batteries and SCs, resp.) of the HESS that can simultaneously meet the demanded power during charging/discharging. This is shown in Figure 11:

$$E_{\text{BAT}} = \frac{P_{\text{BATlimit}D}}{R_{\text{BAT\_}D}}$$
$$E_{\text{BAT}} = \frac{P_{\text{BATlimitC}}}{R_{\text{BAT\_}C}}. \quad (18)$$

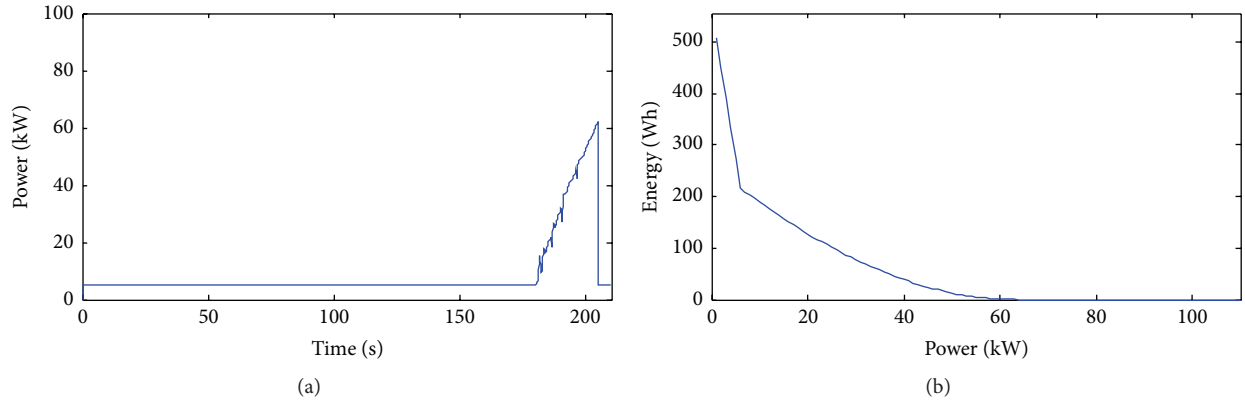

Figure 8: Demanded power in EV mode and corresponding PE function.

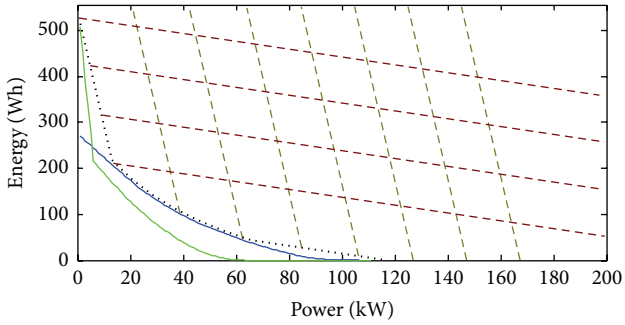

Figure 9: Range of parameter points for the performance of the HESS that meet the demanded power when discharging.

In Figure 11, the blue and green lines mark the selection range of (E_{BAT}, E_{UC}) which is determined by the parameter point for discharging/charging performance. Based on these two lines, the selection range of (E_{BAT}, E_{UC}) that simultaneously meets the demand during charging/discharging is determined and is indicated by the white area at the right side of the thick dotted line ABCD.

It should be noted that, in Figure 11, the lines for the charging/discharging of the battery coincided after (18) are used to perform coordinate transformation. At point A, E_{BAT} is 0, meaning that the SC is acting as the ESS of the HEV. At point D, E_{UC} is 0, meaning that the battery is acting as the ESS of the HEV. Any point within the white area, such as point E, would be able to meet the demanded power for both charging/discharging. There would always be a point F on line ABCD, which has the same abscissa but a smaller ordinate than that of point E. Therefore, point F could be used as the design reference for the HESS that is able to meet the demanded power; however, it simultaneously requires SCs with much smaller capacity. This illustrates that, based on the volume, mass, and cost considerations, the optimal (E_{BAT}, E_{UC}) should be located on line ABCD. The cost, mass, and volume of the HESS when using batteries and SCs of various capacities are then obtained by using the respective energy price, energy mass, and energy volume ratios for the battery and SC as stated in Table 5. This is shown in

$$\begin{aligned} \text{Price} &= \frac{E_{\text{Bat}}}{10} + \frac{E_{\text{UC}}}{1.4}, \\ \text{Weight} &= \frac{E_{\text{Bat}}}{14.6} + \frac{E_{\text{UC}}}{1.36}, \\ \text{Volume} &= \frac{E_{\text{Bat}}}{0.26} + \frac{E_{\text{UC}}}{0.032}. \end{aligned} \tag{19}$$

The results of the mass, volume, and cost of the HESS using battery of different capacity on line ABCD are calculated and are shown in Figure 12.

It can be observed from Figure 12 that when the battery capacity range is 0.6–1 kWh, the weight, volume, and cost of the system are almost minimum values. Compared with the use of either battery or SC as the ESS of the HEVs, the mass, volume, and cost of the ESS are reduced by 30%–50%. The point F (0.8 kWh, 130 Wh) is used as the basis for optimization design of parameters of the HESS. This method is described in the next subsection.

4.3. Optimal Design of the HESS. The energy capacity of a single battery unit is 2.6 Wh (Table 3). The battery package requires 0.8 kWh of energy capacity; therefore, 308 battery units are required. Based on the principle that the voltage of the battery package does not exceed the SC package, a configuration of 77 joints of units in series and four strings in parallel is adopted to form the battery package. The open-circuit voltage of the battery package is 246.4 V.

The energy capacity of a single SC unit is 0.45 Wh (Table 4). The SC package requires 130 Wh of energy capacity; therefore, 289 SC units are required. Using the same principle stated above, the design of the SC package uses 150 joints of units in series. Two strings are laid in parallel, meaning that the SC package comprises 300 units.

The cost, mass, price, and other results of the HESS based on the configuration stated are listed in Table 6. The HESS is designed using the same method and using the following

Table 6: Parameters of the HESS.

	HESS F	HESS A	HESS B	HESS C	Battery D
Single unit of super-capacitor	300 (150 ∗ 2)	1200 (150 ∗ 8)	600 (150 ∗ 4)	150 (150 ∗ 1)	0
Single unit of battery	308 (77 ∗ 4)	0	112 (56 ∗ 2)	616 (77 ∗ 8)	1368 (76 ∗ 18)
Mass/kg	176.08	384	221.12	208.16	355.68
Volume/L	154.44	396	218.16	160.38	246.24
Cost/$	7280	16800	9520	8260	13680

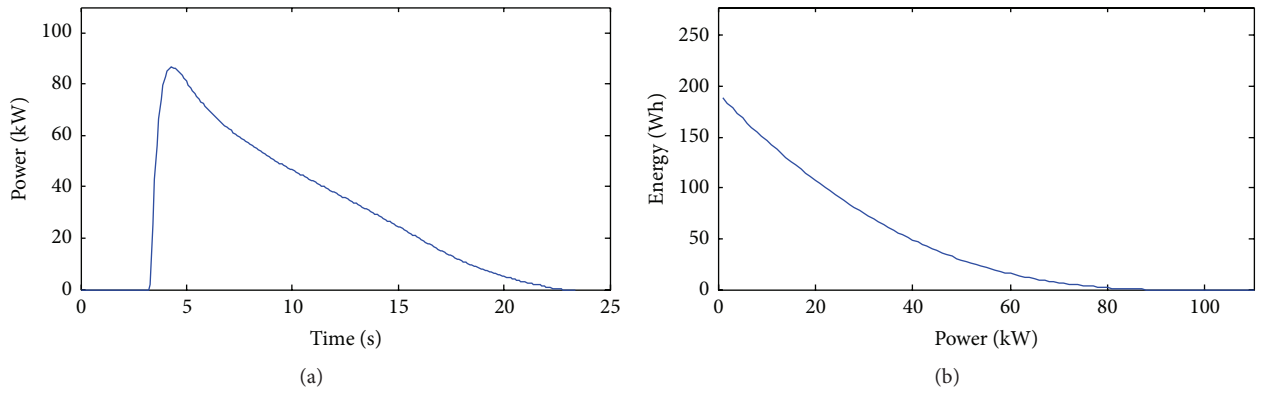

Figure 10: Demanded power and PE function for the regenerative braking process.

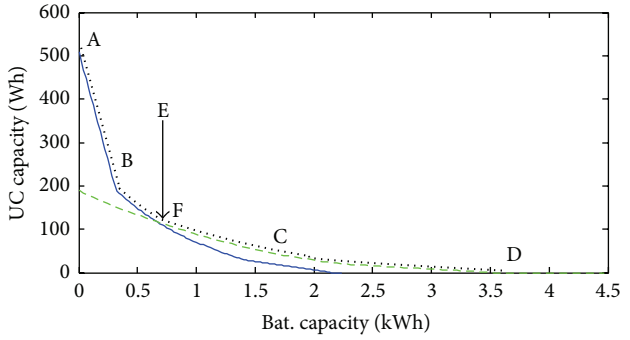

Figure 11: Selection range of (E_{BAT}, E_{UC}) that meets the demand.

points as the bases in Figure 11: A (0 kWh, 508 Wh); B (0.29 kWh, 238 Wh); C (1.6 kWh, 50 Wh); and D (3.55 kWh, 0 Wh). After optimization, there are significant advantages (30%–50%) in terms of the mass, volume, and cost for the HESS.

5. Simulation Test to Validate the Performance

The parameters of the battery and SC package are calculated using the single unit parameters of the SCs and batteries, which are listed in Table 7.

The internal resistance model for the battery and SC package is established using parameters stated in Table 7. The relationships between the DC/DC input and output voltages

Table 7: Parameters of the battery and SC package.

Parameter	SC package	Battery package
Capacity	20 F	32 Ah
Open-circuit voltage/V	340.5	246.4
Internal resistance/mΩ	35.25	134.75
Energy capacity for charging and discharging/Wh	135	800.8
Power limit for charging and discharging/kW	219.6/169.2	19.2/39.4

and currents are used to establish the DC/DC transformer model, which is shown in

$$I_{out}U_{out} = \theta I_{in}U_{in}, \tag{20}$$

where I_{out} and U_{out} represent the DC/DC output current and voltage, respectively; I_{in} and U_{in} represent the DC/DC input current and voltage respectively; and θ represents the DC/DC transfer efficiency. The corresponding DC/DC control strategy model is established simultaneously. This model, along with the models for the DC/DC converter, battery package, and SC package, forms the model for the HESS. This is shown in Figure 13.

The load model is established on the basis of the demanded power under the above three operating conditions (EV, acceleration, and regenerative brake mode). The load model is then used to validate the performance of the HESS through simulation. The results are shown in Figure 14.

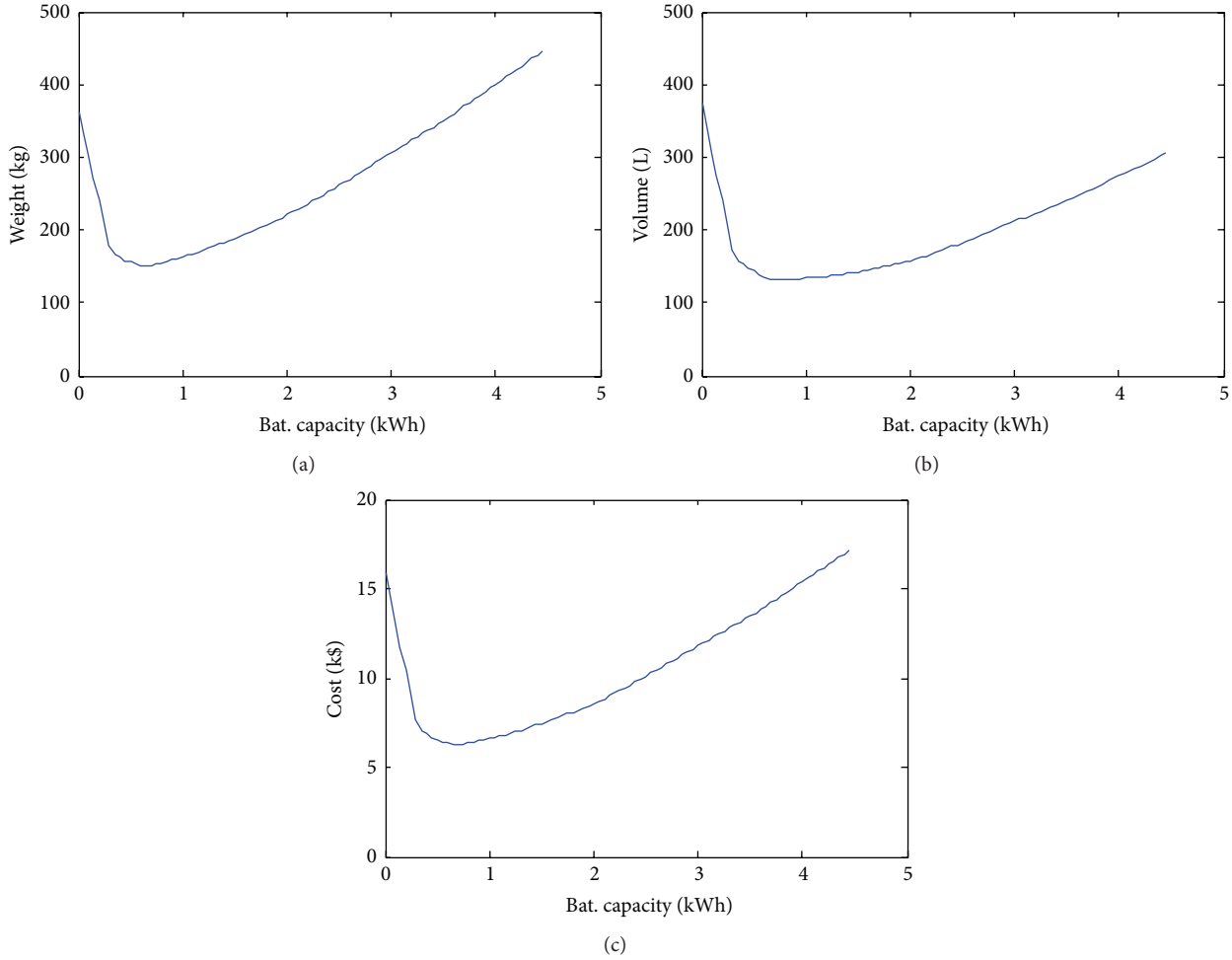

Figure 12: Mass, volume, and cost of the HESS.

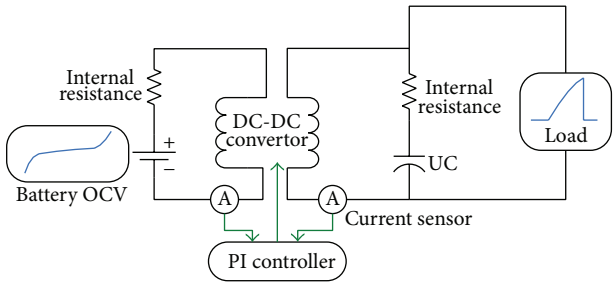

Figure 13: Simulation model for the HESS.

During the simulation, a DC/DC converter is used to control the current of battery in the range of −80 to 160 A. This is to ensure that the battery power could be controlled within its power limit range. Based on the demanded power for the two operating conditions: acceleration and powering up in EV mode, the voltage of the HESS at the load end decreases from the initial 340.5 V to 259 V and 279 V, respectively, whereas the battery SOC decreases from the initial 50% to 48.1% and 44.7%, respectively (Figures 14(a) and 14(b)). For regenerative braking, the voltage at the load end increases from 340.5 V to 393 V, whereas the battery SOC increases from 50% to 51% (Figure 14(c)).

The voltage of the HESS does not exceed 250–400 V during the simulation, while the battery SOC and power are within their limits. The simulation shows that the proposed method based on the PE function could meet the design requirement.

Further, the simulation results of the energy capacity for the SC and battery package during the operation can be verified with each other in Figure 11. The demand power for HESS (E_{BAT}, E_{UC}) under the three operating conditions (acceleration, braking, and powering up in EV mode) is labeled as C1, C2, and C3, respectively (Figure 15).

When point F (0.8 kWh, 135 Wh) is used to design the HESS, the demanded power for SC package under the three operating conditions could be observed on the position of the intersections between C1, C2, and C3 and the line FG, respectively. The length from the intersections between C1/C2/C3 and FG to point G occupies 91%, 92%, and 48% of the total length of FG, respectively. This shows that, to meet the demanded power during acceleration, braking, and powering up in EV mode, the SC package has to supply 91%, 92%, and 44% of the energy capacity, respectively.

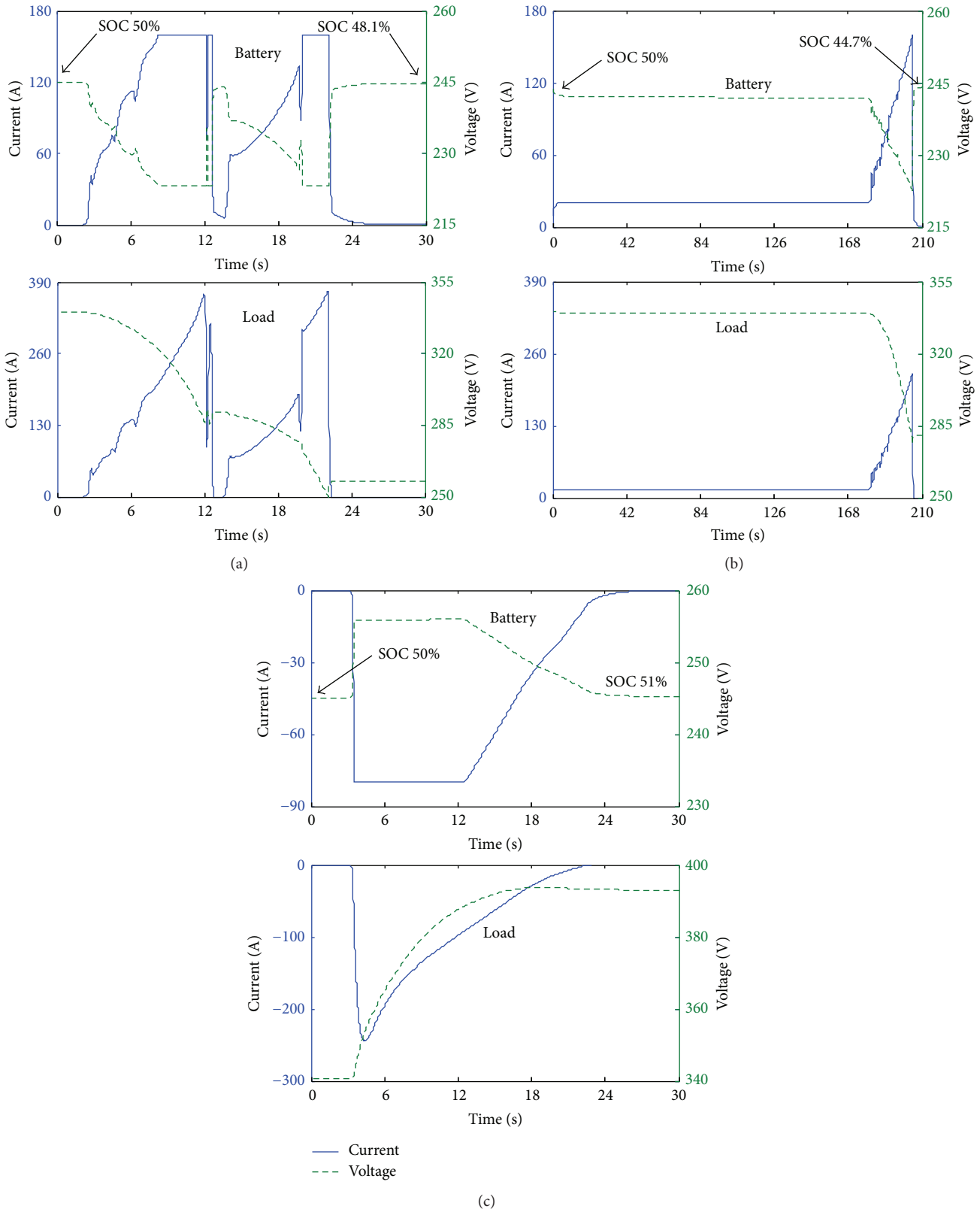

Figure 14: Currents and voltages of the HESS at the load end and battery end based on the demanded power during (a) acceleration; (b) powering up in EV mode; and (c) regenerative braking.

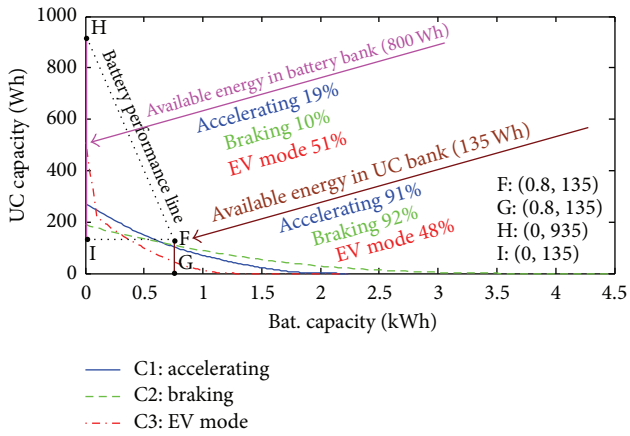

FIGURE 15: Demand for (E_{BAT}, E_{UC}) under the three operating conditions.

Similarly, the demanded power for the battery package under the three operating conditions can be observed from the intersections between C1, C2, and C3 and the line HI, respectively. The length from the intersections between C1, C2, and C3 and HI to point I is 19%, 10%, and 51% of the total length of HI, respectively. This shows that, to meet the demanded power during acceleration, braking, and powering up in EV mode, the battery package has to supply 19%, 10%, and 51% of the energy capacity respectively.

The results of the analysis fit well with the simulation results, thereby validating the proposed design method for the HESS.

6. Conclusion

This paper adopts the concept of the PE function to establish quantitatively mathematical relationship between the battery/SC parameters and HEV demanded power. Based on the three modes (EV, acceleration, and regenerative braking), power and energy capacity are used as design gist for HESS configuration. Taking a hybrid bus as model, this paper calculates the power limit of each power source in HEVs with efficiency consideration. The energy capacity of a single battery unit is 2.6 Wh (Table 3). If battery package requires 0.8 kWh for energy capacity, 308 battery units are required. According to the mathematical methodology, transfer the time-power function into PE function. With PE function and relationship mentioned above, this paper analyzes the demanded power, mass, volume, and cost of HESS and formats mathematical model which contributes to the optimal HESS configuration. F (0.8 kWh,130 Wh) could get the best matching on aspects of mass, volume, and cost compared to A (0 kWh, 508 Wh), B (0.29 kWh, 238), C (1.6 kWh, 50 Wh), and D (3.55 kWh, 0 Wh). Then HESS can be designed for optimization based on analysis results. Battery package constitutes 77 joints of Li-ion battery cells in series and four strings in parallel, while SC package contains 150 joints of capacitor units in series and two strings in parallel. Finally, simulation verifies the optimized HESS that has met the demanded power. F (0.8 kWh, 135 Wh) could meet the power requirements in three driving modes, which is consistent with the foregoing analysis results. Furthermore, the calculation method is the HESS configuration theory which could guide the practice engineering of HESS design for new energy vehicles.

Future work will focus on the degradation model of battery and verification of real vehicle performance.

Conflict of Interests

The authors declare that there is no conflict of interests regarding the publication of this paper.

Acknowledgment

The authors gratefully acknowledge the financial support from the National Natural Science Foundation of China (51107052).

References

[1] S. M. Lukic, J. Cao, R. C. Bansal, F. Rodriguez, and A. Emadi, "Energy storage systems for automotive applications," *IEEE Transactions on Industrial Electronics*, vol. 55, no. 6, pp. 2258–2267, 2008.

[2] M. A. Hannan, F. A. Azidin, and A. Mohamed, "Hybrid electric vehicles and their challenges: a review," *Renewable and Sustainable Energy Reviews*, vol. 29, pp. 135–150, 2014.

[3] L. Solero, A. Lidozzi, V. Serrao, L. Martellucci, and E. Rossi, "Ultracapacitors for fuel saving in small size hybrid vehicles," *Journal of Power Sources*, vol. 196, no. 1, pp. 587–595, 2011.

[4] A. C. Baisden and A. Emadi, "Advisor-based model of a battery and an ultra-capacitor energy source for hybrid electric vehicles," *IEEE Transactions on Vehicular Technology*, vol. 53, no. 1, pp. 199–205, 2004.

[5] D. Hoelscher, A. Skorcz, Y. M. Gao, and M. Ehsani, "Hybridized electric energy storage systems for hybrid electric vehicles," in *Proceedings of the IEEE Vehicle Power and Propulsion Conference (VPPC '06)*, pp. 1–6, IEEE, Windsor, Canada, September 2006.

[6] M. Masih-Tehrani, M.-R. Ha'iri-Yazdi, V. Esfahanian, and H. Sagha, "Development of a hybrid energy storage sizing algorithm associated with the evaluation of power management in different driving cycles," *Journal of Mechanical Science and Technology*, vol. 26, no. 12, pp. 4149–4159, 2012.

[7] S. Williamson, A. Khaligh, S. Oh, and A. Emadi, "Impact of energy storage device selection on the overall drive train efficiency and performance of heavy-duty hybrid vehicles," in *Proceedings of the IEEE Vehicle Power and Propulsion Conference (VPPC '05)*, pp. 381–390, 2005.

[8] J. M. Miller and G. Sartorelli, "Battery and ultracapacitor combinations—where should the converter go?" in *Proceedings of the IEEE Vehicle Power and Propulsion Conference (VPPC '10)*, pp. 1–7, September 2010.

[9] R. E. Araújo, R. De Castro, C. Pinto, P. Melo, and D. Freitas, "Combined sizing and energy management in EVs with batteries and supercapacitors," *IEEE Transactions on Vehicular Technology*, vol. 63, no. 7, pp. 3062–3076, 2014.

[10] P. Sharma and T. S. Bhatti, "A review on electrochemical double-layer capacitors," *Energy Conversion and Management*, vol. 51, no. 12, pp. 2901–2912, 2010.

[11] N. Omar, M. Daowd, P. van den Bossche et al., "Rechargeable energy storage systems for plug-in hybrid electric vehicles-assessment of electrical characteristics," *Energies*, vol. 5, no. 8, pp. 2952–2988, 2012.

[12] N. T. Nguyen, H. V. Ho, S.-T. Hong, and F. Bien, "Smart in-wheel generator using adaptive DC-DC converter for rechargeable batteries in electric vehicles," *International Journal of Precision Engineering and Manufacturing*, vol. 15, no. 6, pp. 1009–1013, 2014.

[13] J. Furukawa, T. Takada, D. Monma, and L. T. Lam, "Further demonstration of the VRLA-type UltraBattery under medium-HEV duty and development of the flooded-type UltraBattery for micro-HEV applications," *Journal of Power Sources*, vol. 195, no. 4, pp. 1241–1245, 2010.

[14] M.-E. Choi, J.-S. Lee, and S.-W. Seo, "Real-time optimization for power management systems of a battery/supercapacitor hybrid energy storage system in electric vehicles," *IEEE Transactions on Vehicular Technology*, vol. 63, no. 8, pp. 3600–3611, 2014.

[15] Z. Fu, B. Wang, X. Song, L. Liu, and X. Wang, "Power-split hybrid electric vehicle energy management based on improved logic threshold approach," *Mathematical Problems in Engineering*, vol. 2013, Article ID 840648, 9 pages, 2013.

[16] R. M. Schupbach, J. C. Balda, M. Zolot, and B. Kramer, "Design methodology of a combined battery-ultracapacitor energy storage unit for vehicle power management," in *Proceedings of the 34th IEEE Annual Power Electronics Specialist Conference (PESC '03)*, vol. 1, pp. 88–93, IEEE, June 2003.

[17] L. Gao, R. A. Dougal, and S. Liu, "Power enhancement of an actively controlled battery/ultracapacitor hybrid," *IEEE Transactions on Power Electronics*, vol. 20, no. 1, pp. 236–243, 2005.

[18] L. Piris-Botalla, G. G. Oggier, A. M. Airabella, and G. O. García, "Power losses evaluation of a bidirectional three-port DC–DC converter for hybrid electric system," *International Journal of Electrical Power and Energy Systems*, vol. 58, pp. 1–8, 2014.

[19] S. Lu, K. A. Corzine, and M. Ferdowsi, "A new battery/ultracapacitor energy storage system design and its motor drive integration for hybrid electric vehicles," *IEEE Transactions on Vehicular Technology*, vol. 56, no. 4, pp. 1516–1523, 2007.

[20] J. M. Miller, P. J. McCleer, M. Everett, and E. G. Strangas, "Ultracapacitor plus battery energy storage system sizing methodology for HEV power split electronic CVT's," in *Proceedings of the IEEE International Symposium on Industrial Electronics*, vol. 1, pp. 317–324, Dubrovnik, Croatia, June 2005.

[21] A. Santucci, A. Sorniotti, and C. Lekakou, "Power split strategies for hybrid energy storage systems for vehicular applications," *Journal of Power Sources*, vol. 258, pp. 395–407, 2014.

[22] E. Ferg, C. Rossouw, and P. Loyson, "The testing of batteries linked to supercapacitors with electrochemical impedance spectroscopy: a comparison between Li-ion and valve regulated lead acid batteries," *Journal of Power Sources*, vol. 226, pp. 299–305, 2013.

[23] Z. Y. Song, H. Hofmann, J. Q. Li, J. Hou, X. B. Han, and M. G. Ouyang, "Energy management strategies comparison for electric vehicles with hybrid energy storage system," *Applied Energy*, vol. 134, pp. 321–331, 2014.

[24] B. Vulturescu, R. Trigui, R. Lallemand, and G. Coquery, "Implementation and test of a hybrid storage system on an electric urban bus," *Transportation Research Part C: Emerging Technologies*, vol. 30, pp. 55–66, 2013.

[25] F. J. Jimenez-Espadafor, J. J. R. Marín, J. A. B. Villanueva, M. T. García, E. C. Trujillo, and F. J. F. Ojeda, "Infantry mobility hybrid electric vehicle performance analysis and design," *Applied Energy*, vol. 88, no. 8, pp. 2641–2652, 2011.

[26] E. Vinot, R. Trigui, and B. Jeanneret, "A complete set of tools for hybrid vehicle design: from cybernetic model to Hardware in the loop simulation," in *Proceedings of the Advances in Hybrid Powertrain International Conference*, pp. 25–26, 2008.

[27] Y.-H. Hung and C.-H. Wu, "An integrated optimization approach for a hybrid energy system in electric vehicles," *Applied Energy*, vol. 98, pp. 479–490, 2012.

[28] Z. Song, J. Q. Li, X. Han et al., "Multi-objective optimization of a semi-active battery/supercapacitor energy storage system for electric vehicles," *Applied Energy*, vol. 135, pp. 212–224, 2014.

[29] N. Hatwar, A. Bisen, H. Dodke, A. Junghare, and M. Khanapurkar, "Design approach for electric bikes using battery and super capacitor for performance improvement," in *Proceedings of the 16th International IEEE Conference on Intelligent Transportation Systems: Intelligent Transportation Systems for All Modes (ITSC '13)*, pp. 1959–1964, October 2013.

[30] Z. Y. Song, H. Hofmann, J. Q. Li, X. B. Han, and M. G. Ouyang, "Optimization for a hybrid energy storage system in electric vehicles using dynamic programing approach," *Applied Energy*, vol. 139, pp. 151–162, 2015.

[31] M. Conte, A. Genovese, F. Ortenzi, and F. Vellucci, "Hybrid battery-supercapacitor storage for an electric forklift: a life-cycle cost assessment," *Journal of Applied Electrochemistry*, vol. 44, no. 4, pp. 523–532, 2014.

[32] X. D. Qu, Q. N. Wang, and Y. B. Yu, "Power demand analysis and performance estimation for active-combination energy storage system used in hybrid electric vehicles," *IEEE Transactions on Vehicular Technology*, vol. 63, pp. 3128–3136, 2014.

[33] M. Averbukh, S. Lineykin, and A. Kuperman, "Portable ultracapacitor-based power source for emergency starting of internal combustion engines," *IEEE Transactions on Power Electronics*, vol. 30, no. 8, pp. 4283–4290, 2015.

[34] R. Sadoun, N. Rizoug, P. Bartholumeüs, B. Barbedette, and P. Lemoigne, "Sizing of hybrid supply (battery-supercapacitor) for electric vehicle taking into account the weight of the additional Buck-Boost chopper," in *Proceedings of the 1st International Conference on Renewable Energies and Vehicular Technology (REVET '12)*, pp. 8–14, IEEE, Hammamet, Tunisia, March 2012.

[35] A. Eddahech, M. Ayadi, O. Briat, and J.-M. Vinassa, "Online parameter identification for real-time supercapacitor performance estimation in automotive applications," *International Journal of Electrical Power & Energy Systems*, vol. 51, pp. 162–167, 2013.

[36] M.-E. Choi, S.-W. Kim, and S.-W. Seo, "Energy management optimization in a battery/supercapacitor hybrid energy storage system," *IEEE Transactions on Smart Grid*, vol. 3, no. 1, pp. 463–472, 2012.

[37] B. Long, S. Lim, Z. Bai, J. Ryu, and K. Chong, "Energy management and control of electric vehicles, using hybrid power source in regenerative braking operation," *Energies*, vol. 7, no. 7, pp. 4300–4315, 2014.

[38] A. Eddahech, O. Briat, M. Ayadi, and J.-M. Vinassa, "Modeling and adaptive control for supercapacitor in automotive applications based on artificial neural networks," *Electric Power Systems Research*, vol. 106, pp. 134–141, 2014.

[39] J. P. Trovão, P. G. Pereirinha, H. M. Jorge, and C. H. Antunes, "A multi-level energy management system for multi-source

electric vehicles—an integrated rule-based meta-heuristic approach," *Applied Energy*, vol. 105, pp. 304–318, 2013.

[40] M. Catelania, L. Ciani, M. Marracci, and B. Tellini, "Analysis of ultracapacitors ageing in automotive application microelectronics reliability," *Microelectronics Reliability*, vol. 5, pp. 1676–1680, 2013.

[41] V. Yuhimenko, M. Averbukh, G. Agranovich, and A. Kuperman, "Dynamics of supercapacitor bank with uncontrolled active balancer for engine starting," *Energy Conversion and Management*, vol. 88, pp. 106–112, 2014.

[42] M. Ayadi, O. Briat, R. Lallemand et al., "Description of supercapacitor performance degradation rate during thermal cycling under constant voltage ageing test," *Microelectronics Reliability*, vol. 54, no. 9-10, pp. 1944–1948, 2014.

[43] B. Vulturescu, R. Trigui, R. Lallemand, and G. Coquery, "Implementation and test of a hybrid storage system on an electric urban bus," *Transportation Research C: Emerging Technologies*, vol. 30, pp. 55–66, 2013.

[44] L. Kumar and S. Jain, "Electric propulsion system for electric vehicular technology: a review," *Renewable and Sustainable Energy Reviews*, vol. 29, pp. 924–940, 2014.